Fyn Deficiency Promotes a Preferential Increase in Subcutaneous Adipose Tissue Mass and Decreased Visceral Adipose Tissue Inflammation

Ting-Wen A. Lee,[1,2] Hyokjoon Kwon,[1] Haihong Zong,[1] Eijiro Yamada,[1,3] Manu Vatish,[4] Jeffrey E. Pessin,[1] and Claire C. Bastie[1,5]

Previous studies have demonstrated that Fyn knockout (FynKO) mice on a standard chow diet display increased glucose clearance and whole-body insulin sensitivity associated with decreased adiposity resulting from increased fatty acid use and energy expenditure. Surprisingly, however, despite a similar extent of adipose tissue (AT) mass accumulation on a high-fat diet, the FynKO mice remained fully glucose tolerant and insulin sensitive. Physiologic analyses demonstrated that the FynKO mice had a combination of skewed AT expansion into the subcutaneous compartment rather than to the visceral depot, reduced AT inflammation associated with reduced T-cell and macrophage infiltration, and increased proportion of anti-inflammatory M2 macrophages. These data demonstrate that Fyn is an important regulator of whole-body integrative metabolism that coordinates AT expansion, inflammation, and insulin sensitivity in states of nutrient excess. These data further suggest that inhibition of Fyn function may provide a novel target to prevent AT inflammation, insulin resistance, and the dyslipidemia components of the metabolic syndrome. *Diabetes* 62:1537–1546, 2013

O besity is the single greatest predictor of the development of type 2 diabetes and has become a global pandemic with 475 million people worldwide affected and with 42% of the U.S. population expected to be obese by 2030 (1). Clinical, epidemiological, and molecular studies have converged to highlight that inflammation is a critical component of obesity-associated insulin resistance (2). Adipose tissue (AT), particularly the visceral AT of obese humans and rodents, is one of the main organs affected by this inflammatory state and is characterized by increased production and secretion of proinflammatory molecules with local and systemic effects (3–6).

At a cellular level, the role of AT macrophages in the pathogenesis of metabolic diseases was evidenced by the increased expression of macrophage markers found in the AT of obese individuals (7,8). Additionally, macrophages within the obese AT display a proinflammatory Th1 polarized M1 phenotype, while, alternatively, activated Th2 polarized M2 macrophages are predominant in the AT of lean animals and humans (9,10), suggesting a switch in macrophage polarization in obese states.

Additionally, evidence has pointed toward the role of other immune cells, such as T cells, in regulating the inflammatory cascades leading to increased proinflammatory M1 macrophages with a much smaller increase or even a reported decrease in anti-inflammatory M2 macrophages (11). Specific subpopulations of T cells play different roles in these processes (11,12), with CD8^{+} T lymphocytes accumulating within the AT of obese individuals (12) and CD4^{+} and particularly Foxp3^{+}CD4^{+} regulatory T cells being decreased in the fat depots of insulin resistant models of obesity (11).

It is interesting to note that metabolic/nutritional signals known to deregulate the insulin pathway and promote insulin resistance in AT also stimulate the inflammatory processes. Activation of macrophages is mediated by the stimulation of Toll-like receptors (TLRs) that sense both microbial agents and nutrients. In particular, TLR4 is directly activated by free fatty acids (13) and TLR4 deficiency in mice protects against diet-induced insulin resistance (14,15). Similarly, signal transduction pathways regulating the energy homeostasis are involved in the activation of T lymphocytes. In particular, the phosphatidylinositol 3-kinase/Akt pathway that stimulates the mammalian target of rapamycin has recently emerged as a regulator of T-cell proliferation and function (16). In addition, liver kinase B1 (LKB1)-deficient and AMP-activated protein kinase (AMPK)-deficient mice have increased T-cell activation and alteration of cytokine expression leading to diet-induced insulin resistance (17).

Fyn is a member of the Src family of nonreceptor tyrosine kinases with diverse biological functions including the regulation of mitogenic signaling and cell cycle entry, proliferation, integrin-mediated interactions, reproduction and fertilization, axonal guidance, and differentiation of oligodendrocytes and keratinocytes (18). Importantly, Fyn has extensively been described for its role in the immune function. Fyn positively regulates mast cell responsiveness (19) and is involved in the differentiation of natural killer cells (20). Moreover, B- and T-cell clonal expansion is partially affected in the Fyn knockout (FynKO) mice and appears to involve Lck, another member of the Src kinase family (21,22).

Notwithstanding its immunological functions, Fyn also plays an important role in the control of metabolism and insulin signaling. Fyn localizes into the lipid rafts of the

plasma membrane (23,24) and interacts with c-Cbl (25) and IRS1 (26), which are important components of the insulin transduction signal (27). More importantly, we have reported that the FynKO mice display a marked reduction in adiposity, reduced fasting glucose and insulin levels, and markedly improved insulin sensitivity (28). The lack of Fyn also results in improved plasma and tissue triglycerides levels, higher energy expenditure, and enhanced fatty acid oxidation. These metabolic characteristics are consequences of Fyn-dependent regulation of LKB1 and AMPK activity in skeletal muscle and AT (29).

The decreased adiposity of the FynKO mice is thought to be responsible for the increased insulin sensitivity demonstrated in these mice on a standard chow diet (28). To explore the effects of a high-fat diet (HFD) on the regulation of insulin biological responsiveness and metabolic regulation in the FynKO mice, we have undertaken a systemic investigation of the metabolic phenotype of FynKO mice maintained on a 60% (kilocalories) HFD for 10 weeks. Remarkably, HFD induced a similar extent of fat mass gain in the FynKO and control mice, yet the FynKO mice remained protected against dyslipidemia, glucose intolerance, and insulin resistance. This metabolic protection against diet-induced metabolic deregulation resulted from multiple compensating mechanisms including differential expansion of specific AT depots and reduction of AT inflammation.

RESEARCH DESIGN AND METHODS

pp59^{fyn} knockout mice and their controls were obtained from The Jackson Laboratory (Bar Harbor, ME) and housed in a facility equipped with a 12-h light/dark cycle. Animals were fed either a chow diet (Research Diets, New Brunswick, NJ) containing 75.9% (kilocalories) carbohydrates, 14.7% protein, and 9.4% fat or an HFD containing 20% (kilocalories) carbohydrates, 20%

protein, and 60% fat for 10 weeks. All studies were approved by and performed in compliance with the guidelines of the Yeshiva University Institutional Animal Care and Use Committee.

Fyn tyrosine kinase activity and Western blotting. Activity was determined with a universal tyrosine kinase activity assay kit (Takara Bio, Shiga, Japan) as recently described in a previous study (30). Tissues were homogenized using a BulletBlender (Next Advance, Averill Park, NY) in a Nodinet P40 (NP-40) lysis buffer containing protease and phosphatase inhibitors. Homogenates were centrifuged for 15 min at 13,000g at 4°C, and supernatants were collected. Protein samples (40 μg) were separated on 10% reducing polyacrylamide gels and electroblotted onto Immobilon-P polyvinylidene difluoride membranes. Immunoblots were blocked with 5% milk in Tris-buffered saline for 2 h at room temperature and incubated overnight at 4°C with the indicated antibodies in Tris-buffered saline and 0.05% Tween 20 (TBST) containing 1% BSA. Blots were washed in TBST and incubated with horseradish peroxidase–conjugated secondary antibodies (1:30,000) for 30 min at room temperature. Membranes were washed in TBST, and antigen-antibody complexes were visualized by chemiluminescence using an enhanced chemiluminescence kit (Pierce, Rockford, IL).

Glucose tolerance test. Chow diet– and HFD-fed control and FynKO animals were fasted for 12 h, and 1 g/kg ᴅ-glucose was administered by oral gavage. Blood was collected from the lateral vein of the tail prior to and at the indicated times after glucose administration. Glucose was measured using a Precision Q.I.D glucometer (MediSense; Abbott Laboratories, Abbott Park, IL).

Euglycemic-hyperinsulinemic clamps. Surgeries to insert the indwelling catheters were performed 4 days prior to the euglycemic-hyperinsulinemic clamp studies as previously described (28,31). Briefly, HFD-fed WT and FynKO mice were fasted for 12 h. The 2-h euglycemic-hyperinsulinemic-clamp was conducted with a continuous infusion of human insulin (4 mU/kg/min; Eli Lilly) and a variable infusion of 25% glucose solution to maintain plasma glucose at 150 mg/dL. Insulin-stimulated whole-body glucose metabolism was assessed with a continuous infusion of ³H-glucose (0.1 μCi/min). To determine insulin-stimulated tissue-specific glucose uptake, 2-deoxy-(ᴅ-1-¹⁴C)-glucose was administrated as a bolus 75 min after the start of the clamp. Blood samples were taken prior to and every 10 min throughout the clamp. Steady state was defined when changes of glucose concentration and infusion rates were stable between 10 and 20% of the target level (150 mg/dL). Glucose infusion rate (millimoles per kilogram per minute) was determined for each time point,
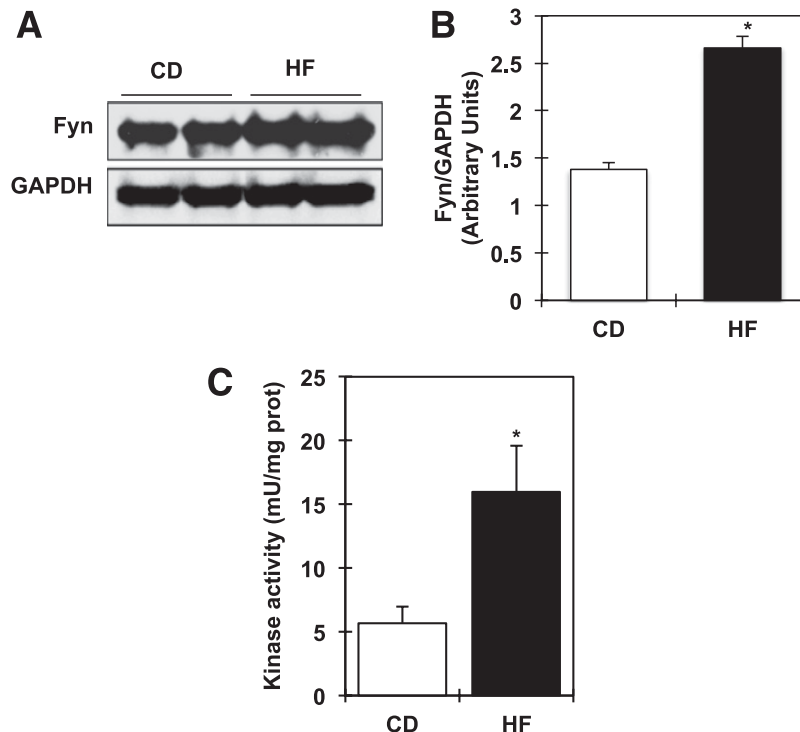

FIG. 1. Fyn kinase expression and activity are increased in the visceral AT during HFD. *A–C*: Age-matched (8 weeks old) male FynKO and WT mice were placed on a standard chow diet (CD) or a 60% (kcal) HFD for 10 weeks. Animals were killed, and Fyn protein expression (*A*) and kinase activity (*C*) in epididymal AT were determined. *B*: Signal quantification of the expression levels Fyn kinase protein corrected by expression levels of glyceraldehyde-3-phosphate dehydrogenase (GAPDH) protein. prot, protein.

and average was calculated for the last 30 min of the clamp. At the end of the clamp, tissue samples were collected and frozen at −80°C for the measurement of glucose uptake and hepatic glucose production.

Analysis of plasma parameters. Mice were anesthetized with pentobarbital (50 mg/kg), and cardiac puncture was performed. Blood was centrifuged for 10 min at 9,000g at 4°C. Plasma was collected. Basal insulin levels, triglycerides, and nonesterified fatty acids (NEFAs) were quantified using an insulin ELISA kit (Mercodia, Winston Salem, NC), Infinity kit (Thermo Fisher Scientific, Waltham, MA), and the HR series NEFA assay (Wako Diagnostics, Richmond, VA), respectively. Plasma tumor necrosis factor (TNF)-α levels were determined using an ELISA kit from R&D (Minneapolis, MN).

Total body mass and magnetic resonance imaging. Total body mass was recorded every 7 days at 1500 h. For determination of fat mass, animals were placed in a clear plastic holder without anesthesia or sedation and inserted into the EchoMRI-3-in-1 system from Echo Medical Systems (Houston, TX).

Microcomputed tomography. Mice under deep anesthesia (2% isoflurane) were scanned in an in vivo microcomputed tomography scanner. Noise was removed from the computed tomography images using a Gaussian filter. Fat distribution was analyzed from the hip-femoral joint to a landmark at the distal end of the lung.

Immunohistochemical staining. Immunohistochemistry was performed using the Biomodule IHC staining kit from Invitrogen (Carlsbad, CA). Briefly, 10-μm serial sections were dewaxed and epitope retrieval was performed by immerging the slides into a citrate buffer at 100°C for 20 min. Slides were incubated with a macrophage-specific marker F4/80 antibody. Sections were counterstained with hematoxylin-eosin.

Quantitative PCR analysis. Epididymal fat pads were homogenized into QIAzol Lysis Reagent (Qiagen, Valencia, CA). For macrophages isolated from WT and FynKO stromal vascular fractions (SVFs), SVF cells were stained with phycoerythrin-labeled anti-mouse F4/80 antibody and macrophages were sorted using anti-phycoerythrin antibody–labeled magnetic beads (Miltenyi Biotec, Auburn, CA). Total RNA was isolated using RNeasy Mini Kit (Qiagen Sciences) and reverse transcribed to cDNA using the SuperScript VILO cDNA synthesis kit (Invitrogen). TaqMan (Applied Biosystems, Branchburg,
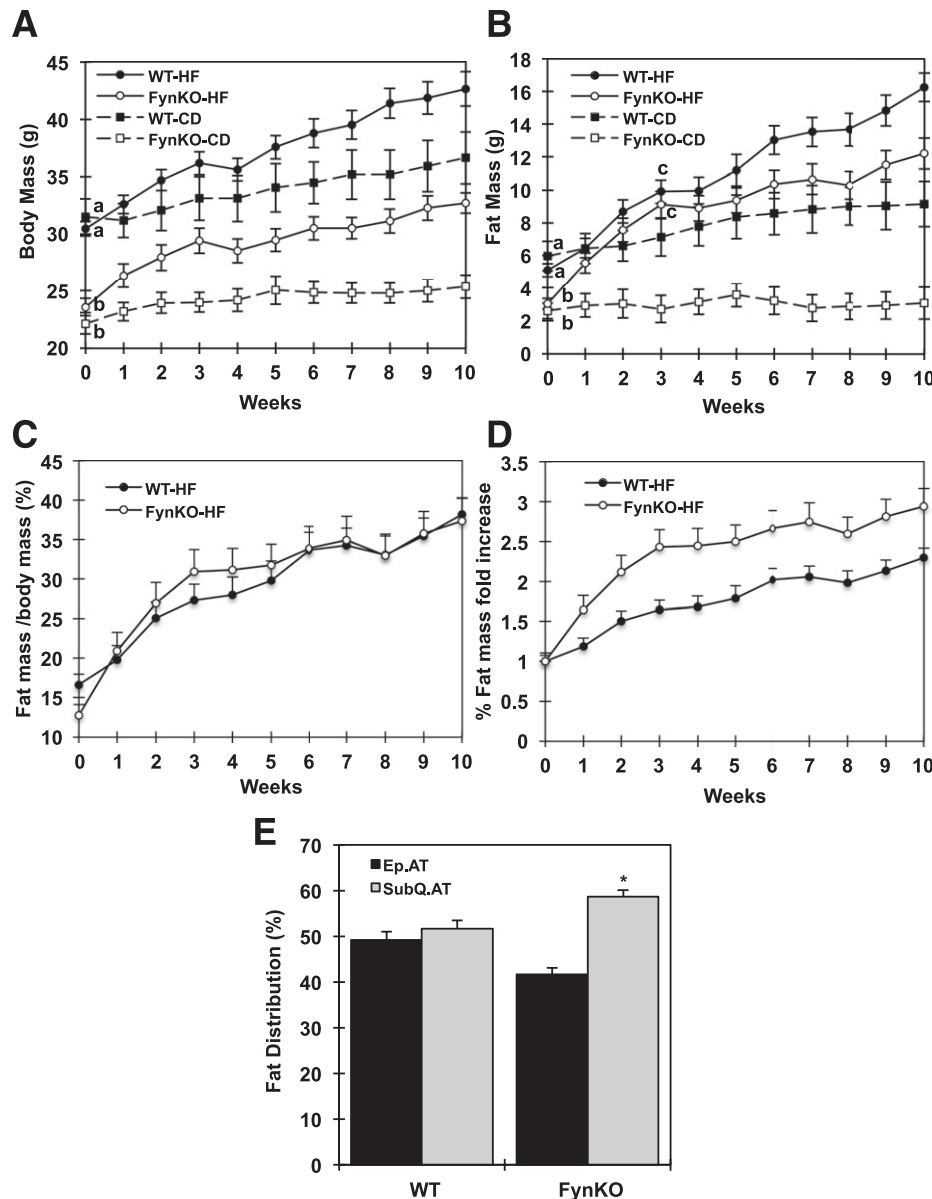

FIG. 2. HFD-fed FynKO mice display an increase in body weight and fat mass similar to that observed in WT mice. *A* and *B*: Age-matched (8 weeks old) male FynKO and WT mice were placed on a standard chow diet (CD) or a 60% (kcal) HFD (HF) for 10 weeks. Total body weight (*A*) and total fat mass (*B*) were determined on a weekly basis. *C* and *D*: Fat mass percentage (fat mass per total body mass) (*C*) and fat mass percentage fold increase (*D*) were determined on a weekly basis in HFD-fed FynKO and WT mice. *E*: Percentage fat mass distribution in visceral (epididymal [Ep.AT]) and subcutaneous (inguinal [SubQ.AT]) adipose depots of the FynKO and WT mice. Data are expressed as means ± SEM (*n* = 6 animals/group). Identical letters indicate values that are not statistically different from each other (*P* > 0.05). *P < 0.05 vs. WT.

NJ) RT-PCR was performed for measurement of mRNA of F4/80, CCL2, TNF-α, interleukin (IL)-6, IL-10, and other markers of M1 and M2 macrophages (Nos2, chitinase 3-like3, and arginase 1). Relative expression levels of the mRNAs were determined using standard curves.

SVF preparation. Minced ATs (pieces <10 mg) were placed in HEPES-buffered Dulbecco's modified Eagle's medium supplemented with 10 mg/mL BSA and centrifuged at 1,000*g* for 10 min to precipitate erythrocytes and other blood cells. AT samples were treated with 0.05 mg/mL liberase (Liberase TM Research Grade; Roche Applied Science, Indianapolis, IN) and incubated at 37°C for 20 min. Samples were passed through a sterile 250-μm nylon mesh. The suspension was centrifuged at 1,000*g* for 5 min. The precipitated cells (SVF) were resuspended in erythrocyte lysis buffer. The erythrocyte-depleted SVF cells were centrifuged at 500*g* for 5 min. The pellet was resuspended in fluorescence-activated cell sorter buffer.

Flow cytometry analysis. Cells were stained with phycoerythrin-labeled anti-mouse F4/80, allophycocyanin (APC)-labeled anti-mouse CD11c, phycoerythrin-labeled anti-mouse CD3, fluorescein isothiocyanate–labeled anti-mouse CD4, and APC-labeled anti-mouse CD8a (BD Pharmingen, San Diego, CA). For identification of regulatory CD4^{+} T cells, cells were stained with PerCP-labeled anti-mouse CD4 and APC-labeled anti-mouse CD25 antibodies, fixed and permeabilized using a Cytofix/Cytoperm kit (BD Pharmingen), and stained with fluorescein isothiocyanate–labeled anti-Foxp3 (eBioscience, San Diego, CA). 7-aminoactinomycin D was used to exclude dead cells.

Statistics. Results are expressed as means ± SEM. The data were analyzed by one-way ANOVA followed by post hoc analysis for comparisons between individual groups. Differences were considered statistically significant at a level of $P < 0.05$.

RESULTS

FynKO mice are not protected against HFD-induced weight gain. Chow diet–fed FynKO mice display reduced adiposity with increased fatty acid oxidation, energy expenditure, and insulin sensitivity (28). Interestingly, Fyn protein expression (Fig. 1*A* and *B*) and tyrosine kinase activity (Fig. 1*C*) were increased by approximately two- to threefold in the epididymal AT of HFD-fed control mice, suggesting that Fyn could play a role in the etiology of diet-induced obesity and/or insulin resistance.

For investigation of the functional role of Fyn in HFD-induced obesity, control and FynKO mice were fed a 60% HFD for 10 weeks. Although FynKO mice total body mass remained significantly lower than that of the control mice, FynKO mice total body weight was increased by 40% in response to the HFD (Fig. 2*A*); a similar percent increase also occurred in control mice. This unexpected result was consistent with a significant increase in total fat mass (Fig. 2*B*). Although fat mass percentage was initially 25% lower in the FynKO mice (12 vs. 16%), it quickly increased in response to HFD and reached values similar to those of the control mice (Fig. 2*C*). Consequently, fat mass percentage fold increase in the FynKO mice was actually significantly higher than for the control mice (Fig. 2*D*). Additionally, body fat distribution assessed by microcomputed tomography revealed that fat mass was equally distributed between the epididymal (visceral) and inguinal (subcutaneous) AT depots in HFD-fed control mice. In contrast, HFD-fed FynKO mice had a greater preference for subcutaneous fat storage compared with visceral (Fig. 2*E*). Fat preferential distribution into the subcutaneous storage remained remarkably higher in the HFD-fed FynKO mice than in weight-matched control mice on chow diet (Supplementary Fig. 1*A*). Interestingly, phosphorylation levels of AMPK and one of its downstream targets, acetyl-CoA carboxylase (ACC), remained elevated in the epididymal AT of the HFD-fed FynKO mice (Supplementary Fig. 1*B*). In contrast, AMPK was increased to a very small extent with no significant effect on ACC phosphorylation levels in the FynKO mice subcutaneous fat depots compared with the control mice (Supplementary Fig. 1*B* and *C*), which, in

part, may account for the disproportionate increase of the subcutaneous AT in the FynKO mice.

FynKO mice on HFD remained glucose tolerant and insulin sensitive. As previously reported, FynKO mice fed a chow diet demonstrated lower plasma fasting glucose, reduced insulin levels, and decreased triglycerides and NEFAs (28). These parameters were increased in HFD-fed FynKO mice but remained lower than in the HFD-fed control mice and in fact still were in the range of age-matched chow diet–fed control mice (Table 1). As previously reported (28), chow diet–fed FynKO mice displayed increased glucose clearance compared with chow diet–fed control mice. More importantly, while in HFD-fed control mice glucose clearance was impaired, it was only mildly altered in HFD-fed FynKO mice (Fig. 3*A* and *B*). Remarkably, glucose clearance remained significantly better in the HFD-fed FynKO mice compared with both HFD-fed and chow diet–fed control mice, as evidenced by lower blood glucose levels during a glucose tolerance test (Fig. 3*A*) and lower area under the curve values (Fig. 3*B*).

For determination of insulin sensitivity and tissue-specific insulin action, euglycemic-hyperinsulinemic clamp experiments were conducted in HFD-fed FynKO and control mice. Glucose levels were initially higher in the control mice than in the FynKO mice, and steady state was reached by 60 min of glucose infusion (Supplementary Fig. 2*A* and *B*). Steady-state insulin levels were lower in the FynKO mice (Table 2), suggesting a higher insulin clearance. However, despite this, the glucose infusion rate was greatly increased in the FynKO mice (Fig. 3*C*), demonstrating enhanced whole-body insulin sensitivity in the FynKO mice. Moreover, AT (Fig. 3*D*) and skeletal muscle (Fig. 3*E*) glucose uptake rates were higher in the FynKO mice and insulin-induced suppression of hepatic glucose production was increased in the FynKO mice (Supplementary Fig. 2*C*). Interestingly, glucose uptake values observed in the HFD-fed FynKO animals remained similar to those usually obtained for chow diet–fed control animals (data not shown), suggesting that insulin sensitivity was essentially fully conserved in the FynKO mice. In line with this, Akt phosphorylation levels after clamp were significantly higher in the epididymal AT (Fig. 3*F*) and the skeletal muscle (Fig. 3*G*) of the FynKO mice.

TABLE 1

Plasma parameters of control (WT) and FynKO mice on standard (chow) and HFD diets

Glucose (mg/dL)	Chow	60% HFD
WT	124 ± 12[a]	193 ± 5.7[c]
FynKO	71 ± 1.1[b]	111 ± 7.6[a]
Insulin (ng/dL)		
WT	51 ± 3.9[a]	386 ± 37[c]
FynKO	31 ± 9.9[b]	73 ± 9.4[d]
Triglycerides (mg/dL)		
WT	58 ± 7.6[a]	88 ± 12[c]
FynKO	36 ± 2.2[b]	51 ± 5.7[a]
NEFA (mmol/L)		
WT	0.52 ± 0.06[a]	0.74 ± 0.03[c]
FynKO	0.29 ± 0.06[b]	0.67 ± 0.04[d]

Age-matched (8 weeks old) male FynKO and control (WT) mice were placed on a standard chow diet or a 60% (kcal) HFD for 10 weeks. Fasting plasma glucose, insulin, triglycerides, and NEFAs were determined. The data were analyzed by one-way ANOVA. [a,b,c,d]Identical letters indicate values that are not significantly different.
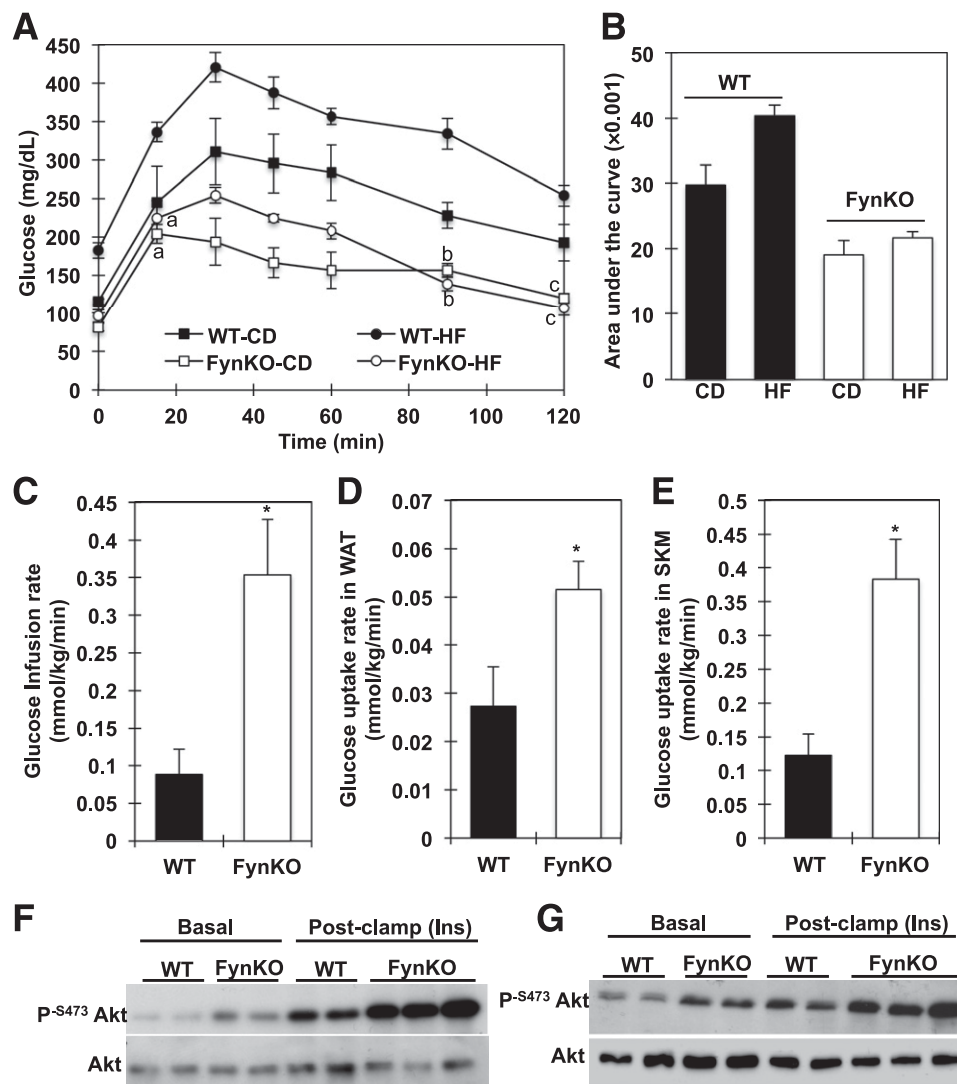
FIG. 3. FynKO mice are protected against HFD-induced glucose intolerance and insulin (Ins) resistance. *A*: FynKO and WT were maintained either on a standard chow diet (CD) or on an HFD (HF) for 10 weeks and were fasted for 12 h before receiving 1 g/kg D-glucose via oral gavage. Blood glucose levels were measured at the indicated time points. Data are expressed as means ± SEM (*n* = 5 animals per group). Identical letters indicate values that are not statistically different from each other (*P* > 0.05). *B–D*: FynKO and WT mice were maintained on an HFD for 10 weeks and fasted for 12 h before being subjected to a nonstressed conscious euglycemic-hyperinsulinemic clamp. *B*: Whole-body infusion rate. *C*: Insulin-stimulated glucose uptake in epididymal AT. *D*: Insulin-stimulated glucose uptake in skeletal muscle. Phosphorylation levels (S473) of Akt were determined in the epididymal AT (*E*) and skeletal muscle (SKM) (*F*) of WT and FynKO mice before (no insulin) and after (insulin) euglycemic-hyperinsulinemic clamp. Data are expressed as means ± SEM (*n* = 4 [WT] and 4 [FynKO]). P, phosphorylated. *$P < 0.05$ vs. WT.

FynKO mice on HFD display reduced AT inflammation. Elevated levels of TNF-α have been reported in various diabetic and insulin resistant states (32). Interestingly, plasma TNF-α levels were lower in HFD-fed FynKO mice compared with their more insulin resistant controls (Fig. 4*A*). Consistent with this, mRNA expression of TNF-α was twofold lower in the epididymal AT of FynKO mice (Fig. 4*B*). Additionally, the gene expression of both macrophage chemoattractant *CCL2* and macrophage marker F4/80 was also reduced in the epididymal fat pads of the FynKO mice (Fig. 4*B*). This suggested a reduced macrophage presence within the AT of the FynKO mice that could explain the apparent decrease in systemic inflammation. However, the expression of the anti-inflammatory cytokine IL-10 was dramatically reduced in the FynKO mice AT (Fig. 4*C*).

FynKO on HFD have reduced AT macrophage and T-cell content. Consistent with the mRNA expression,

immunohistochemical analysis of epididymal fat pads revealed that adipocytes of control mice were surrounded by F4/80-positive macrophages referred to as crown-like structures (Fig. 5*A*). In contrast, very few crown-like structures were found in the AT of the FynKO mice (Fig. 5*A*).

AT is composed of adipocytes and other cells (including macrophages and T cells) termed the SVF. For investigation of whether the immune cell populations within the SVF of the FynKO epididymal AT were altered, macrophage subpopulations were first analyzed using macrophage-specific markers. Consistent with the reduced F4/80 mRNA expression in the epididymal fat pad (Fig. 4*B*), numbers of F4/80-positive cells were reduced, suggesting that macrophage numbers were decreased in the SVF of the FynKO mice (Fig. 5*B*). More importantly, within the isolated F4/80 positive cell fraction, numbers of CD11c⁻ cells (anti-inflammatory M2 phenotype) were significantly

TABLE 2
Euglycemic-hyperinsulinemic clamp data for control (WT) and FynKO mice on HFD

	WT	FynKO
Basal glucose (mmol/L)	10.5 ± 1.6	4.8 ± 1.7*
Clamp glucose (mmol/L)	7.4 ± 1.3	6.0 ± 1.00
Basal insulin (pmol/L)	664 ± 63	126 ± 47*
Clamp insulin (pmol/L)	880 ± 20	207 ± 44*
GIR (mmol/kg/min)	0.09 ± 0.03	0.35 ± 0.07*
GIR/insulin ([mmol/kg/min]/[pmol/L])	1.01 ± 0.3	17.7 ± 1.3*

Age-matched male FynKO and control (WT) mice were placed on an HFD (60% kcal) for 10 weeks. Basal and clamp glucose and insulin levels were determined. Glucose infusion rate (GIR) and glucose infusion rate/insulin were calculated. *$P < 0.05$ vs. WT HFD.

higher than those of CD11c$^+$ cells (inflammatory M1 phenotype) in FynKO mice (Fig. 5C and D). Consistently, M1 macrophage markers Nos2 and proinflammatory cytokine IL-6 were decreased (Fig. 5E), while M2 macrophage markers arginase 1 and Ym1/chitinase 3-like3 were significantly increased in the SVF of the FynKO mice (Fig. 5F). This suggested that the immune balance within the AT of the FynKO mice was skewed to the M2 macrophages.

Additionally, numbers of CD3$^+$ T cells were markedly reduced in the epididymal AT of FynKO mice (Fig. 6). The similar numbers of CD3$^+$ T cells found in spleens of FynKO and control mice (Fig. 6B) suggested that the apparent decrease in T-cell numbers did not result from a peripheral decrease of this cellular population but, rather, was a consequence of a reduced T-cell recruitment within the AT. Interestingly, CD8$^+$ T-cell fraction was decreased by 50% in the AT of FynKO mice (Fig. 6C). However, the CD4$^+$ T-cell fraction remained similar in the AT of both FynKO and control mice (Fig. 6D). The proportion of Foxp3$^+$CD25$^+$CD4$^+$ T regulatory cells in the epididymal AT of FynKO and control mice was similar (Fig. 6E). However, total cell numbers of T regulatory cells in FynKO mice were much lower than those of control mice owing to reduced numbers of CD4$^+$ T cells in FynKO mice (Fig. 6F). Since Foxp3$^+$CD4$^+$T regulatory cells are a major source for the production of the anti-inflammatory cytokine IL-10, these data account for the reduced levels of IL-10 in the AT of the HFD-fed FynKO mice.

DISCUSSION

We previously demonstrated that Fyn is a negative regulator of fatty acid oxidation through the inhibition of AMPK in skeletal muscle and white AT (28). The FynKO mice display enhanced fatty acid use and AMPK activity in the AT and skeletal muscle, associated with increased energy expenditure. As a result, Fyn-deficient animals are
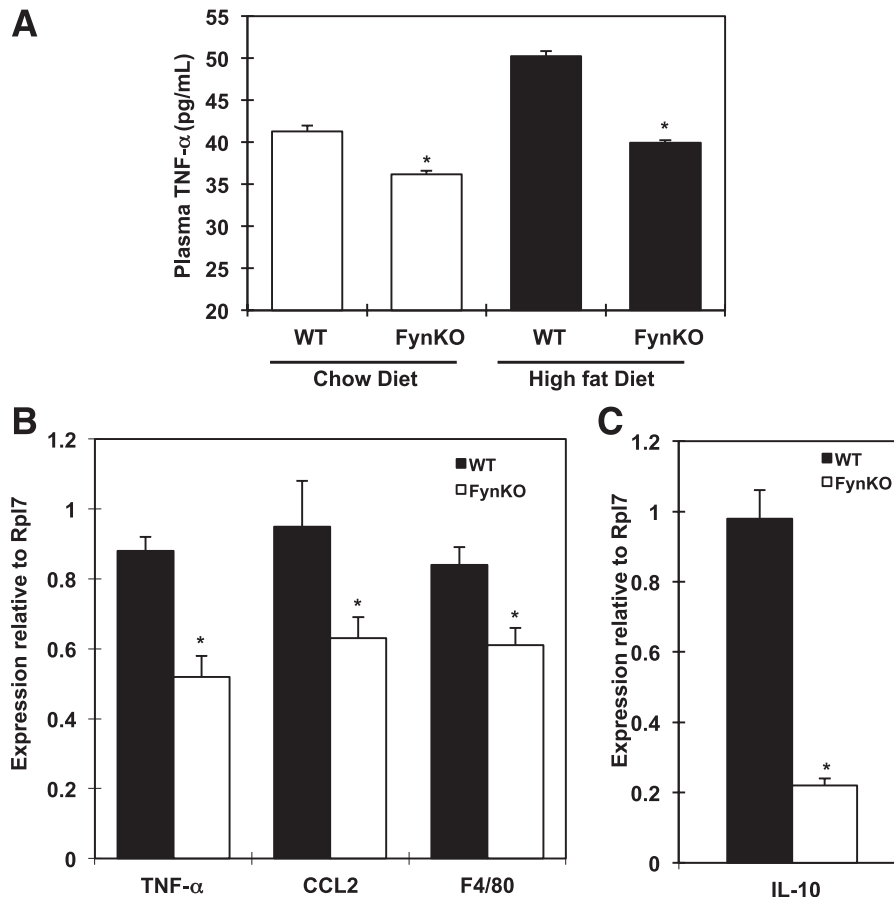

FIG. 4. FynKO mice are protected against HFD-induced AT inflammation. FynKO and control (WT) mice were fed a chow diet or an HFD for 10 weeks. A: Plasma TNF-α levels. B: Expression levels of TNF-α, CCL2, and F4/80 mRNA in epididymal AT of HFD-fed WT and FynKO mice. C: Expression levels of IL-10 mRNA in epididymal AT of HFD-fed WT and FynKO mice. Data are expressed as means ± SEM (n = 5 animals/group). *$P < 0.05$ vs. WT.
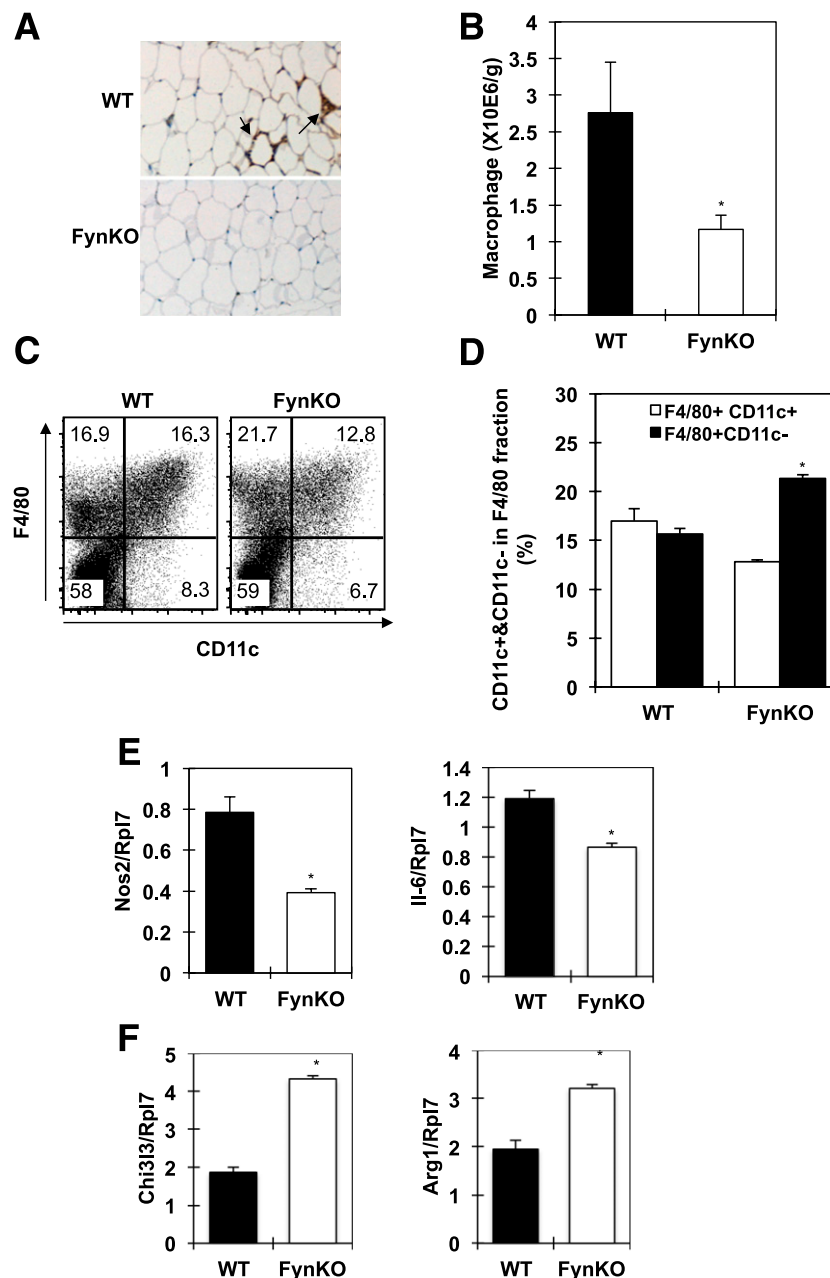
FIG. 5. FynKO mice are resistant to HFD-induced accumulation of proinflammatory M1 macrophages in AT. FynKO and control (WT) mice were fed an HFD for 10 weeks. *A*: Representative image of F4/80 staining of epididymal AT of WT (*upper panel*) and FynKO (*lower panel*) mice. Black arrows indicate crown-like structures. *B*: Numbers of F4/80-positive cells in the SVF of epididymal AT determined by flow cytometry. *C*: Representative fluorescence-activated cell sorter profile of proinflammatory M1 (F4/80$^+$CD11c$^+$) and anti-inflammatory M2 (F4/80$^+$CD11c$^-$) macrophages in the SVF of epididymal AT. *D*: Proportion of proinflammatory M1 (F4/80$^+$CD11c$^+$) and anti-inflammatory M2 (F4/80$^+$CD11c$^-$) macrophages in the SVF of epididymal AT of WT and FynKO mice. *E* and *F*: Macrophages were sorted from SVF of epididymal AT of HFD-fed WT and FynKO mice. *E*: Expression of M1 macrophage markers in sorted macrophages. *F*: Expression of M2 macrophage markers in sorted macrophages. Data are expressed as means ± SEM. (*n* = 3–4 animals/group.) *$P < 0.05$ vs. WT. (A high-quality color representation of this figure is available in the online issue.)

lean and show reduced adiposity. Interestingly, chow diet–fed FynKO mice are also characterized by increased glucose clearance and whole-body insulin sensitivity.

The observation that obesity is associated with a low-grade inflammation process in AT suggested a relationship between fat cells and the immune system (33). Interestingly, Fyn has been extensively described in the immunology field, and lack of Fyn alters the development or clonal expansion of several immune cell lineages (19–22,34). However, whether Fyn has a role in diet-induced

AT inflammation has not been investigated. In this study, we analyzed the effects of HFD on the metabolic profile and the relationship between insulin sensitivity and inflammation in the FynKO mice.

Unexpectedly, FynKO mice were not protected against diet-induced weight gain. However, plasma triglyceride levels, although increased after HFD, remained significantly lower in the FynKO mice (25 vs. 40% increase), demonstrating that dyslipidemia was only moderate in the HFD-fed FynKO mice. Although the FynKO mice gained
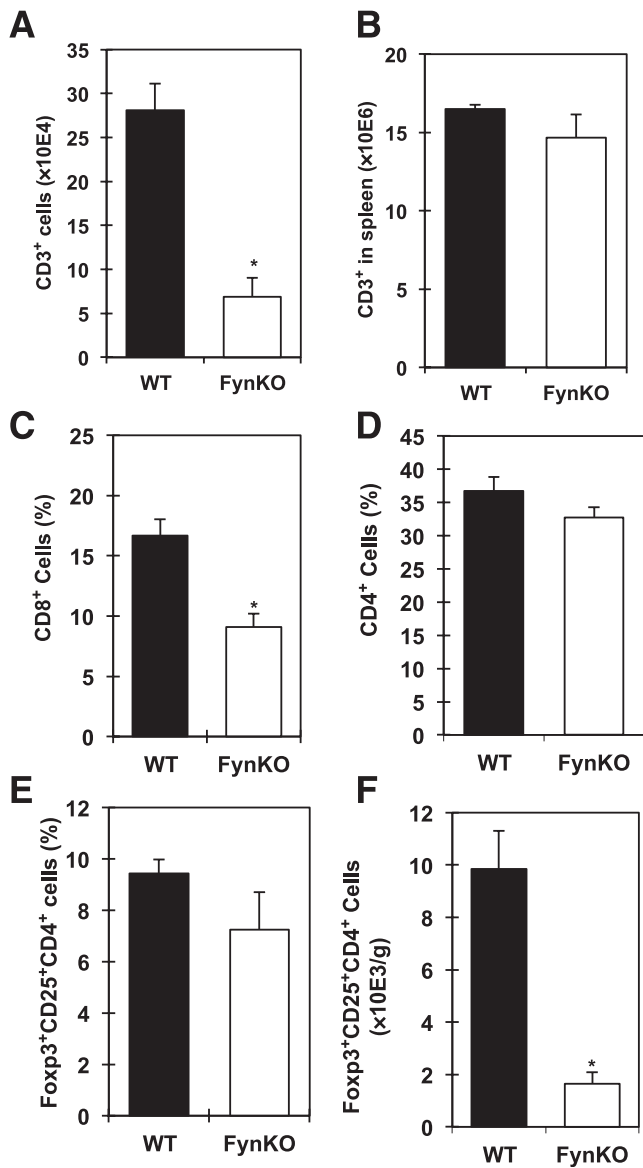
FIG. 6. FynKO mice maintained on an HFD have a reduced T-lymphocyte population in AT. FynKO and control (WT) mice were fed HFD for 10 weeks. *A*: Total number of CD3$^+$ T cells in the epididymal AT was determined by flow cytometry. *B*: Total number of CD3$^+$ T cells in the spleen. *C*: Proportion of CD8$^+$ T cells among the CD3$^+$ T-cell population in the epididymal AT. *D*: Proportion of CD4$^+$ T cells among the CD3$^+$ T-cell population in the epididymal AT. *E*: Proportion of Foxp3$^+$CD25$^+$ (T regulatory) cells among the CD4$^+$ T-cell population in the epididymal AT. *F*: Total number of Foxp3$^+$CD25$^+$ (T regulatory) cells in the epididymal AT. Data are expressed as means ± SEM (*n* = 4 animals/group). *$P < 0.05$ vs. WT.

proportionally more fat mass than the control mice (Fig. 2*D*), they significantly remained smaller than the control mice, which could per se influence the insulin sensitivity. To address this issue, we compared the glucose tolerance between weight-matched HFD-fed FynKO mice and chow diet–fed control mice (Fig. 3*A*). Glucose tolerance was improved in the HFD-fed FynKO mice, indicating that enhanced glucose clearance and insulin sensitivity in the FynKO are independent of their size or adiposity. This is consistent with our previous report demonstrating that Fyn heterozygous animals, displaying only 5% difference in body mass compared with controls, also display improved glucose clearance (28).

Increased adiposity is associated with insulin resistance; however, functional AT is also necessary to maintain adequate insulin sensitivity, as lipodystrophic models develop severe insulin resistance (35). AT expansion ability appears to be as important as the absolute amount of AT to correct obesity-related metabolic problems. Visceral and subcutaneous adipose depots have different tissue expansion abilities that correlate with their roles in the establishment of metabolic complications (36–38). The greater expansion capacity of the subcutaneous depot is consistent with its protective role against diet-induced insulin resistance (39–41). Interestingly, although the FynKO mice show a significant fat mass increase, the distribution was shifted to the subcutaneous depot. Consistent with the preventive effects of this AT depot, the FynKO mice did not show any impairment of insulin sensitivity. Differences in the AMPK pathway in the two fat depots could, partly, explain the preferential fat accumulation in the subcutaneous depot. The increased AMPK and ACC phosphorylation levels in the visceral AT could limit fat accumulation in this depot, while the excess dietary fat would be redirected to the subcutaneous depot. Consistently, triglyceride levels in the HFD-fed FynKO mice skeletal muscle were significantly decreased (Supplementary Fig. 3), suggesting that oxidation is likely to stay elevated in this tissue. Therefore, the higher lipid-buffering levels due to the fat accumulation in the subcutaneous depot, combined with increased oxidation, could possibly explain the lower circulating lipid levels observed in the FynKO mice.

However, once the maximal expandability is reached, metabolic complications are likely to occur. As such, larger adipocytes display altered secretory functions leading to modifications of the adipocyte-secreted proteins. This is particularly evidenced by increased proinflammatory cytokine secretion, which plays a role in both macrophage recruitment and insulin responsiveness impairment (42). However, despite an apparent AT hypertrophy, the HFD-fed FynKO mice remained insulin responsive. Furthermore, two major cytokines generally associated with insulin resistance, TNF-α and CCL2 (7,32,43,44), were decreased in the AT of the FynKO mice along with lower F4/80 expression levels, which together confirmed the reduced macrophage presence in the FynKO mice epididymal AT. More importantly, analysis of the macrophage population within the SVF of the FynKO mice AT revealed a higher proportion of M2 macrophages, underlining the lower inflammatory state observed in the FynKO mice.

T cells are mediators of the systemic metabolic function. While the CD3$^+$CD8$^+$ T cells allow for the recruitment of macrophages, the CD3$^+$CD4$^+$T cells, particularly the Foxp3$^+$CD25$^+$CD4$^+$ regulatory T cells, secrete the anti-inflammatory cytokine IL-10 that functions to prevent macrophage infiltration (11,12). Counterintuitively, we found decreased IL-10 expression levels in the fat of the FynKO mice that would be expected to result in increased AT inflammation. However, the reduced level of IL-10 is readily accounted for by the overall decreased number of AT Foxp3$^+$CD25$^+$CD4$^+$ regulatory T cells that results from a total reduction in CD3$^+$ T cells and CD8$^+$ T-cell numbers. Interestingly, there was no difference in peripheral CD3$^+$ T-cell numbers, suggesting that the reduced T-cell population was due to defective cell recruitment rather than an alteration of the T-cell development. Thus, despite the reduced level of anti-inflammatory cytokine IL-10, the overall dampening of the innate immune response for both

macrophage and T-cell activation into the AT likely accounts for the dramatic protection against HFD-induced insulin resistance.

Fyn is a major regulator of innate immune responses by relaying the activation of the TLR in macrophages as well as the T-cell receptor in T cells (22). Since fatty acids directly activate both the TLR4 (13) and the T-cell receptor (45), it is possible that lack of Fyn could alter fatty acid–induced inflammatory responses in both T cells and macrophages. However, a recent study has shown that signals sent by the AT itself attract "non-activated" macrophages (46), highlighting the predominant role of this organ in triggering obesity-induced inflammation. In states of obesity, profound metabolic and morphologic alterations of the AT modify the pool of AT-secreted proteins, resulting in the recruitment of immune cells. Several of these adipokines have been identified and functionally characterized; however, it is highly likely that additional factors remain to be discovered. We have demonstrated that Fyn plays an important role in the AT metabolism, and this current study suggests that Fyn could modulate fat distribution and therefore the pool of AT-secreted proteins. For that reason, an alternative mechanism could involve the alteration of signals sent by the AT of the FynKO mice, resulting in the reduced recruitment of immune cells into this organ. Nonetheless, further investigations using pharmacological or tissue-specific modulation of Fyn activity and/or expression will be needed to determine the precise mechanism(s) involved as well as demonstrate whether this will provide protection and/or reversal against HFD-induced insulin resistance and AT inflammation.

REFERENCES

1. Finkelstein EA, Khavjou OA, Thompson H, et al. Obesity and severe obesity forecasts through 2030. Am J Prev Med 2012;42:563–570
2. de Luca C, Olefsky JM. Inflammation and insulin resistance. FEBS Lett 2008;582:97–105
3. Scherer PE. Adipose tissue: from lipid storage compartment to endocrine organ. Diabetes 2006;55:1537–1545
4. Shoelson SE, Lee J, Goldfine AB. Inflammation and insulin resistance. J Clin Invest 2006;116:1793–1801
5. Bosello O, Zamboni M. Visceral obesity and metabolic syndrome. Obes Rev 2000;1:47–56
6. Fantuzzi G. Adipose tissue, adipokines, and inflammation. J Allergy Clin Immunol 2005;115:911–919; quiz 920
7. Weisberg SP, McCann D, Desai M, Rosenbaum M, Leibel RL, Ferrante AW Jr. Obesity is associated with macrophage accumulation in adipose tissue. J Clin Invest 2003;112:1796–1808
8. Xu H, Barnes GT, Yang Q, et al. Chronic inflammation in fat plays a crucial role in the development of obesity-related insulin resistance. J Clin Invest 2003;112:1821–1830
9. Lumeng CN, Bodzin JL, Saltiel AR. Obesity induces a phenotypic switch in adipose tissue macrophage polarization. J Clin Invest 2007;117:175–184
10. Lumeng CN, Deyoung SM, Bodzin JL, Saltiel AR. Increased inflammatory properties of adipose tissue macrophages recruited during diet-induced obesity. Diabetes 2007;56:16–23
11. Feuerer M, Herrero L, Cipolletta D, et al. Lean, but not obese, fat is enriched for a unique population of regulatory T cells that affect metabolic parameters. Nat Med 2009;15:930–939
12. Nishimura S, Manabe I, Nagasaki M, et al. CD8+ effector T cells contribute to macrophage recruitment and adipose tissue inflammation in obesity. Nat Med 2009;15:914–920
13. Lee JY, Sohn KH, Rhee SH, Hwang D. Saturated fatty acids, but not unsaturated fatty acids, induce the expression of cyclooxygenase-2 mediated through Toll-like receptor 4. J Biol Chem 2001;276:16683–16689
14. Shi H, Kokoeva MV, Inouye K, Tzameli I, Yin H, Flier JS. TLR4 links innate immunity and fatty acid-induced insulin resistance. J Clin Invest 2006;116:3015–3025
15. Tsukumo DM, Carvalho-Filho MA, Carvalheira JB, et al. Loss-of-function mutation in Toll-like receptor 4 prevents diet-induced obesity and insulin resistance. Diabetes 2007;56:1986–1998
16. Powell JD, Delgoffe GM. The mammalian target of rapamycin: linking T cell differentiation, function, and metabolism. Immunity 2010;33:301–311
17. MacIver NJ, Blagih J, Saucillo DC, et al. The liver kinase B1 is a central regulator of T cell development, activation, and metabolism. J Immunol 2011;187:4187–4198
18. Saito YD, Jensen AR, Salgia R, Posadas EM. Fyn: a novel molecular target in cancer. Cancer 2010;116:1629–1637
19. Parravicini V, Gadina M, Kovarova M, et al. Fyn kinase initiates complementary signals required for IgE-dependent mast cell degranulation. Nat Immunol 2002;3:741–748
20. Gadue P, Morton N, Stein PL. The Src family tyrosine kinase Fyn regulates natural killer T cell development. J Exp Med 1999;190:1189–1196
21. Palacios EH, Weiss A. Function of the Src-family kinases, Lck and Fyn, in T-cell development and activation. Oncogene 2004;23:7990–8000
22. Salmond RJ, Filby A, Qureshi I, Caserta S, Zamoyska R. T-cell receptor proximal signaling via the Src-family kinases, Lck and Fyn, influences T-cell activation, differentiation, and tolerance. Immunol Rev 2009;228:9–22
23. Mastick CC, Saltiel AR. Insulin-stimulated tyrosine phosphorylation of caveolin is specific for the differentiated adipocyte phenotype in 3T3-L1 cells. J Biol Chem 1997;272:20706–20714
24. Liang X, Nazarian A, Erdjument-Bromage H, Bornmann W, Tempst P, Resh MD. Heterogeneous fatty acylation of Src family kinases with polyunsaturated fatty acids regulates raft localization and signal transduction. J Biol Chem 2001;276:30987–30994
25. Ribon V, Printen JA, Hoffman NG, Kay BK, Saltiel AR. A novel, multifuntional c-Cbl binding protein in insulin receptor signaling in 3T3-L1 adipocytes. Mol Cell Biol 1998;18:872–879
26. Sun XJ, Pons S, Asano T, Myers MG Jr, Glasheen E, White MF. The Fyn tyrosine kinase binds Irs-1 and forms a distinct signaling complex during insulin stimulation. J Biol Chem 1996;271:10583–10587
27. Saltiel AR, Pessin JE. Insulin signaling pathways in time and space. Trends Cell Biol 2002;12:65–71
28. Bastie CC, Zong H, Xu J, et al. Integrative metabolic regulation of peripheral tissue fatty acid oxidation by the SRC kinase family member Fyn. Cell Metab 2007;5:371–381
29. Yamada E, Pessin JE, Kurland IJ, Schwartz GJ, Bastie CC. Fyn-dependent regulation of energy expenditure and body weight is mediated by tyrosine phosphorylation of LKB1. Cell Metab 2010;11:113–124
30. Yamada E, Bastie CC, Koga H, Wang Y, Cuervo AM, Pessin JE. Mouse skeletal muscle fiber-type-specific macroautophagy and muscle wasting are regulated by a Fyn/STAT3/Vps34 signaling pathway. Cell Rep 2012;1:557–569
31. Zong H, Armoni M, Harel C, Karnieli E, Pessin JE. Cytochrome P-450 CYP2E1 knockout mice are protected against high-fat diet-induced obesity and insulin resistance. Am J Physiol Endocrinol Metab 2012;302:E532–E539
32. Hotamisligil GS, Murray DL, Choy LN, Spiegelman BM. Tumor necrosis factor alpha inhibits signaling from the insulin receptor. Proc Natl Acad Sci USA 1994;91:4854–4858
33. Neels JG, Olefsky JM. Inflamed fat: what starts the fire? J Clin Invest 2006;116:33–35

34. Sefton BM, Taddie JA. Role of tyrosine kinases in lymphocyte activation. Curr Opin Immunol 1994;6:372–379

35. Reitman ML, Mason MM, Moitra J, et al. Transgenic mice lacking white fat: models for understanding human lipoatrophic diabetes. Ann N Y Acad Sci 1999;892:289–296

36. Adams M, Montague CT, Prins JB, et al. Activators of peroxisome proliferator-activated receptor gamma have depot-specific effects on human preadipocyte differentiation. J Clin Invest 1997;100:3149–3153

37. Virtue S, Vidal-Puig A. It's not how fat you are, it's what you do with it that counts. PLoS Biol 2008;6:e237

38. Jensen MD. Role of body fat distribution and the metabolic complications of obesity. J Clin Endocrinol Metab 2008;93(Suppl. 1):S57–S63

39. Tran TT, Yamamoto Y, Gesta S, Kahn CR. Beneficial effects of subcutaneous fat transplantation on metabolism. Cell Metab 2008;7:410–420

40. Snijder MB, Dekker JM, Visser M, et al. Associations of hip and thigh circumferences independent of waist circumference with the incidence of type 2 diabetes: the Hoorn Study. Am J Clin Nutr 2003;77:1192–1197

41. Tchoukalova YD, Koutsari C, Karpyak MV, Votruba SB, Wendland E, Jensen MD. Subcutaneous adipocyte size and body fat distribution. Am J Clin Nutr 2008;87:56–63

42. Skurk T, Alberti-Huber C, Herder C, Hauner H. Relationship between adipocyte size and adipokine expression and secretion. J Clin Endocrinol Metab 2007;92:1023–1033

43. Hotamisligil GS, Shargill NS, Spiegelman BM. Adipose expression of tumor necrosis factor-alpha: direct role in obesity-linked insulin resistance. Science 1993;259:87–91

44. Heilbronn LK, Campbell LV. Adipose tissue macrophages, low grade inflammation and insulin resistance in human obesity. Curr Pharm Des 2008;14:1225–1230

45. McMurray DN, Jolly CA, Chapkin RS. Effects of dietary n-3 fatty acids on T cell activation and T cell receptor-mediated signaling in a murine model. J Infect Dis 2000;182(Suppl. 1):S103–S107

46. Oh DY, Morinaga H, Talukdar S, Bae EJ, Olefsky JM. Increased macrophage migration into adipose tissue in obese mice. Diabetes 2012;61:346–354